

---

# RiNALMo: General-Purpose RNA Language Models Can Generalize Well on Structure Prediction Tasks

---

Rafael Josip Penić<sup>1</sup> Tin Vlašić<sup>2</sup> Roland G. Huber<sup>3</sup> Yue Wan<sup>2</sup> Mile Šikić<sup>2</sup>

## Abstract

Ribonucleic acid (RNA) plays a variety of crucial roles in fundamental biological processes. Recently, RNA has become an interesting drug target, emphasizing the need to improve our understanding of its structures and functions. Over the years, sequencing technologies have produced an enormous amount of unlabeled RNA data, which hides important knowledge and potential. Motivated by the successes of protein language models, we introduce RiboNucleic Acid Language Model (RiNALMo) to help unveil the hidden code of RNA. RiNALMo is the largest RNA language model to date with 650 million parameters pre-trained on 36 million non-coding RNA sequences from several available databases. RiNALMo is able to extract hidden knowledge and capture the underlying structure information implicitly embedded within the RNA sequences. RiNALMo achieves state-of-the-art results on several downstream tasks. Notably, we show that its generalization capabilities can overcome the inability of other deep learning methods for secondary structure prediction to generalize on unseen RNA families. The code has been made publicly available on <https://github.com/lbcb-sci/RiNALMo>.

## 1. Introduction

Large language models (LLMs) trained on massive text corpora have been performing remarkably on various natural

language understanding and generation tasks (Devlin et al., 2018; Radford et al., 2018; Raffel et al., 2020; Brown et al., 2020; Touvron et al., 2023; Chowdhery et al., 2023). In recent years, the exploration of language models has gone beyond the domain of natural language processing, reaching into the realms of biology and its data. A vast amount of sequenced protein data provided a ground for training protein language models, and since they have proven to be an extremely valuable asset in protein generative (Ferruz et al., 2022; Madani et al., 2023) and structure prediction tasks (Wu et al., 2022; Lin et al., 2023).

Ribonucleic acids (RNAs) play crucial roles in fundamental biological processes, including transcription, cell signaling, chromatin remodeling, and genome imprinting. Like proteins, RNAs have recently become an attractive drug target, whose function and the way they interact with other biological molecules are closely related to their structure (Childs-Disney et al., 2022; Garner, 2023). However, much less attention has been given to applying language models to RNA-related problems, partly because there is no such amount of available data and corresponding structures, and partly because similar problems tend to be more difficult than for proteins.

Currently, there are only two single-input-sequence RNA foundation models, RNA-FM (Chen et al., 2022) and Uni-RNA (Wang et al., 2023), that found applications and were tested on several structure and function prediction tasks. RNA-FM is a 100 million parameters Transformer encoder based on the original implementation proposed by Vaswani et al. (2017) and trained exclusively on 23.7 million non-coding RNAs (ncRNAs) from the RNACentral database (RNACentral Consortium, 2020). Wang et al. (2023) pre-trained an ensemble of language models ranging from 25 to 400 million parameters trained on a much larger dataset of 1 billion sequences with the architecture analogous to the ESM protein language model (Rives et al., 2021). Unlike the Uni-RNA, RNA-FM is a publicly available RNA foundation model.

Motivated by the recent successes of protein language models and the latest architectural improvements in LLMs, we propose RiNALMo, a novel RNA language model. We pre-trained RiNALMo on a set of carefully curated 36 mil-

<sup>1</sup>Faculty of Electrical Engineering and Computing, University of Zagreb, Zagreb, Croatia <sup>2</sup>Genome Institute of Singapore (GIS), Agency for Science, Technology and Research (A\*STAR), 60 Biopolis Street, Genome, Singapore 138672, Republic of Singapore <sup>3</sup>Bioinformatics Institute (BII), Agency for Science, Technology and Research (A\*STAR), 30 Biopolis Street, Matrix, Singapore 138671, Republic of Singapore. Correspondence to: Rafael Josip Penić <rafael-josip.penic@fer.hr>, Tin Vlašić <tin.vlasic@gis.a-star.edu.sg>, Mile Šikić <mile\_sikic@gis.a-star.edu.sg>.

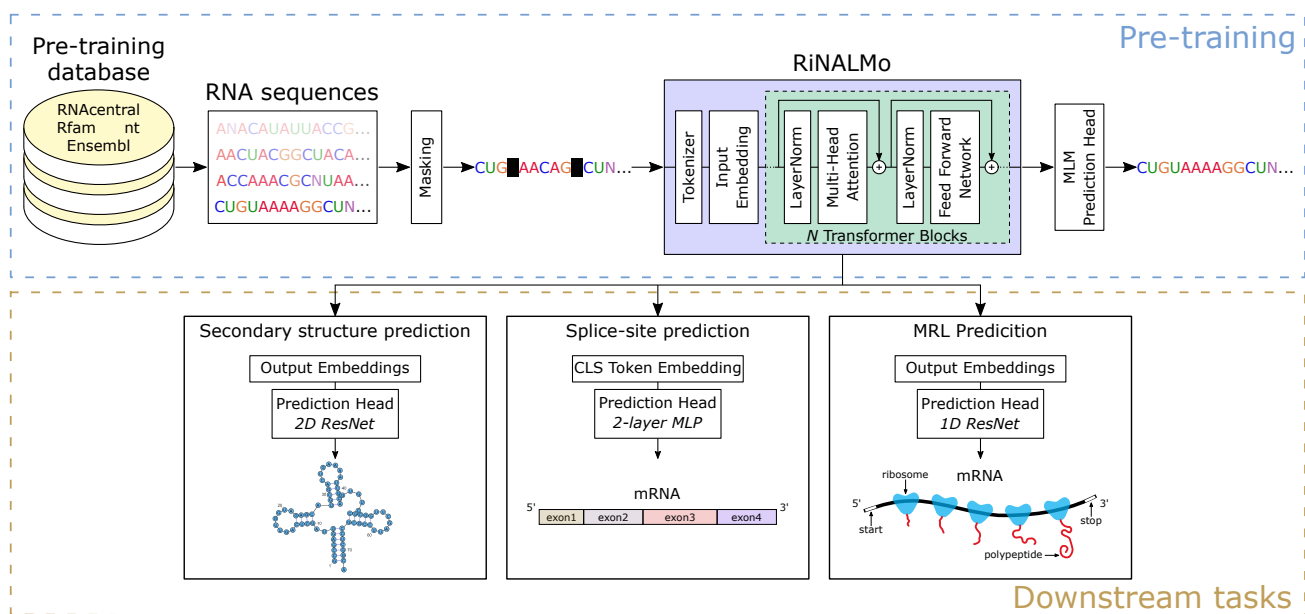


**Figure 1. RiNALMo pre-training and applications.** In the pre-training stage, RiNALMo is trained on unlabeled RNA sequences from several databases using masked language modeling (MLM). The final language model comprises 33 Transformer blocks with the embedding dimension of 1280. Once pre-trained, RiNALMo is separately fine-tuned for several structural and functional downstream tasks in which its expressive output embeddings, utilized by the prediction heads, significantly improve the performance.

lion ncRNA sequences from the RNAcentral database augmented by several other RNA databases. RiNALMo is a 650 million parameters BERT-style Transformer encoder (Devlin et al., 2018) advanced by modern architectural techniques such as rotary positional embedding (RoPE) (Su et al., 2024), SwiGLU activation function (Shazeer, 2020) and FlashAttention-2 (Dao, 2023). During pre-training, RiNALMo is able to extract hidden knowledge and capture the underlying structural information embedded within the sequences at the single-nucleotide level. Later, its output embeddings serve as a powerful sequence representation that, in comparison to other foundation models and state-of-the-art methods, improves the performance on various structural and functional RNA downstream tasks. In particular, RiNALMo shows remarkable generalization capability on secondary structure prediction of RNA families not encountered in the training dataset where other deep learning methods fail. RiNALMo pre-training procedure and downstream tasks are illustrated in Figure 1.

The main contributions of the paper are as follows:

- We propose RiNALMo, a 650 million parameters RNA language model, which is the largest RNA language model to date that can fully leverage the potential of a vast amount of public unannotated RNA sequences;
- We show that the generalization capability of RiNALMo can overcome the problem of other deep learning methods for secondary structure prediction to per-

form well on RNA families not seen in the training dataset;

- We conducted a set of extensive experiments on several RNA structural and functional downstream tasks whose results show that RiNALMo outperforms other RNA language models and deep learning methods on the majority of datasets.

The remainder of the paper is structured as follows. Section 2 presents the related work. In Section 3, we present RiNALMo and describe the dataset it was pre-trained on. In Section 4, we provide quantitative and qualitative assessments of RiNALMo evaluated on structural and several functional downstream tasks. In Section 5, we discuss the most important results and ideas of the paper. Section 6 concludes the paper.

## 2. Related Work

**Protein language models.** Most efforts in applying the ideas originally developed for natural language processing have been focused on proteins after the success of AlphaFold (Jumper et al., 2021) in the prediction of protein structures. A vast amount of publicly available protein sequences has been seen as promising ground for studying generative and predictive models for protein-related biological problems. One of the first papers that applied self-supervised language modeling approaches to protein data

was proposed by Rives et al. (2021). The authors' LLM, ESM-1b, was pre-trained on 250 million protein sequences and tested on several downstream tasks, including the secondary structure and tertiary contact prediction, where it achieved state-of-the-art results. Later on, several other protein LMs were proposed and tested on various downstream tasks (Heinzinger et al., 2019; Nambiar et al., 2020; Brandes et al., 2022; Elnaggar et al., 2022). Protein language models also play an important role in protein tertiary structure prediction. ESM-2 and OmegaPLM are examples of protein LMs that efficiently replace a multiple sequence alignment (MSA) step in ESMFold (Lin et al., 2023) and OmegaFold (Wu et al., 2022), which are deep learning-based structure prediction methods. Furthermore, several papers (Ferruz et al., 2022; Madani et al., 2023; Nijkamp et al., 2023; Chen et al., 2024) proposed language models that can generate protein sequences with specific biophysical properties. Recently, McWhite et al. (2023) showed that protein language models are a powerful new tool for generating MSAs, where the model's output embeddings are leveraged to circumvent the need for many standard components of MSA algorithms.

**RNA foundation models.** Chen et al. (2022) proposed RNA-FM, a BERT-style foundation model based on the original implementation of a Transformer encoder described in (Vaswani et al., 2017). RNA-FM is a 100 million parameters model pre-trained on 23.7 million unannotated ncRNAs from the RNACentral database using the standard masked language modeling (MLM) task. It was used and tested on several structural and functional prediction tasks and found its application in an RNA 3D structure prediction method E2Efold-3D (Shen et al., 2022). A more recent RNA foundation model, Uni-RNA (Wang et al., 2023), was pre-trained on a dataset of 1 billion RNA sequences for a spectrum of structural and functional downstream tasks. The model is a BERT-style Transformer encoder enhanced by several advanced techniques such as RoPE and fused layer norm. The authors pre-trained language models of different sizes and reported when the model parameters exceeded 400M, the performance in downstream tasks reached a plateau with their architectures and datasets. Zhang et al. (2024) proposed an MSA-based RNA language model (RNA-MSM), a BERT-style language model that, instead of a single input sequence, utilizes a set of homologous sequences. RNA-MSM uses RNACmap (Zhang et al., 2021) for an automatic homology search. Its embedding module consists of two position-embedding layers that encode rows and columns of the MSA separately. The authors showed that RNA structure information is preserved in the output attention maps and embeddings of RNA-MSM and that such an approach improves secondary structure prediction. However, obtaining the MSAs is a very time-consuming procedure – it takes RNACmap on average 9 hours to obtain an MSA for one RNA sequence of length 60 (Zhang et al., 2024).

**Language models for specific genomics-related downstream tasks.** Besides the foundation models, several authors proposed language models aimed at solving a few specific downstream tasks. Chen et al. (2023) proposed SpliceBERT, a BERT-style encoder pre-trained exclusively on more than 2 million precursor messenger RNA (pre-mRNA) sequences from different vertebrates for studying RNA splicing. SpliceBERT outperforms DNABERT (Ji et al., 2021), a language model trained only on a human genome for prediction of promoters, splice sites and transcription factor binding sites, both on human and non-human splice-site prediction tasks. It demonstrates the superior performance and better generalization capability of language models pre-trained on multiple species. Later, the authors of DNABERT introduced DNABERT-2 (Zhou et al., 2023), which is a more advanced language model trained on a multi-species genome dataset. Yang et al. (2022) proposed single-cell BERT (scBERT), a BERT-style language model pre-trained on huge amounts of unlabeled single-cell RNA-seq data for cell type annotation. BigRNA (Celaj et al., 2023) is a language model consisting of an ensemble of 7 models pre-trained on the genomes of 70 individuals on a task to predict DNA-matched RNA-seq data. BigRNA accurately predicts tissue-specific RNA expression and the binding sites of proteins and microRNAs.

### 3. RNA Language Model

Our language model is an encoder-only Transformer that focuses on the task of understanding and unveiling the RNA code. At the heart of the model is the self-attention mechanism (Vaswani et al., 2017), which allows the capturing of important local and global contextual information. Before being passed to the Transformer, an RNA sequence is tokenized and turned into a 1280 dimension vector using a learned input embedding model. RiNALMo consists of 33 Transformer blocks, and each block comprises a multi-head attention and a feed-forward network (FFN). The position of the tokens is encoded using the RoPE (Su et al., 2024), which effectively encapsulates both the relative and the absolute positional information. Each multi-head attention has 20 attention heads, which scales the model to 650M parameters. To improve the pre-training efficiency of such a large model, we employed the IO-aware FlashAttention-2 (Dao, 2023), a fast and memory-efficient exact attention. In the FFN, we use two linear layers and the SwiGLU activation function (Shazeer, 2020) which combines the advantages of the Swish activation function and the gated linear unit (GLU). The Transformer modules are interconnected using residual connections. We use the layer normalization put inside the residual blocks to stabilize the training and have well-behaved gradients at initialization (Xiong et al., 2020).

We pre-trained RiNALMo using the MLM where we cor-

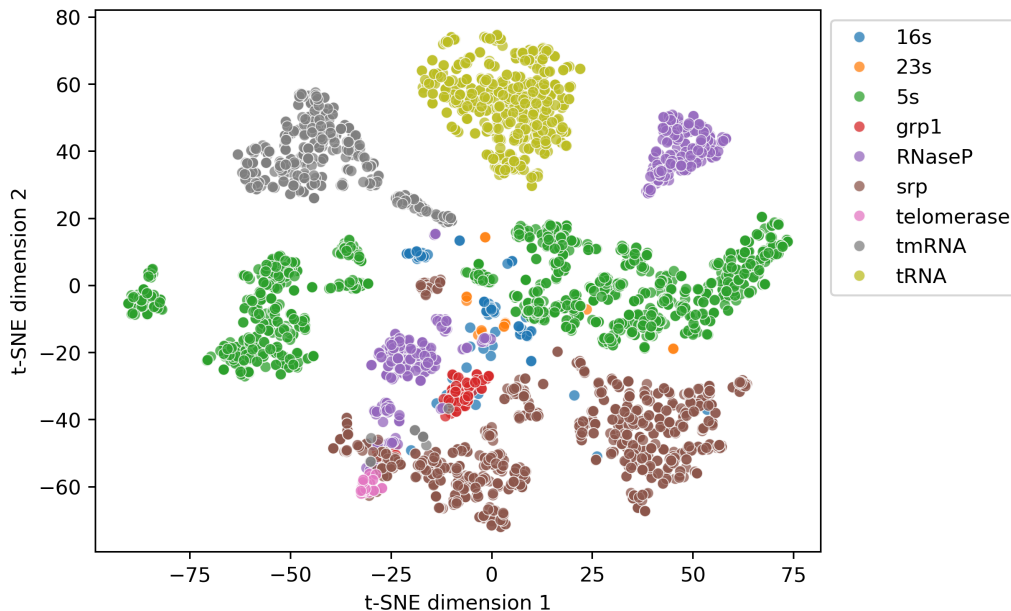


Figure 2. t-SNE visualization of sequence embeddings produced by RiNALMo for RNAs from the inter-family generalization evaluation dataset.

rupted unlabeled RNA sequences and then tasked the model to reconstruct them. In this paper, each nucleotide is a single token. To corrupt the input sequence, we randomly selected 15% of the tokens in the training sequence. Of these, 80% are masked, i.e., replaced with the unique vocabulary token [MASK], 10% are replaced with a randomly selected token from the vocabulary, and the remaining 10% are left intact. We used ordinary cross-entropy training loss function. RiNALMo’s pre-training procedure and architecture are shown in Figure 1. More details on the pre-training and model’s hyperparameters can be found in Appendix A.

Besides using the RNACentral database (RNACentral Consortium, 2020), we collected sequences from Rfam (Kalvari et al., 2020), nt (Sayers et al., 2022) and Ensembl (Martin et al., 2022) as well, making it a pre-training dataset of 36 million unique ncRNA sequences. To ensure sequence diversity in each training batch, we clustered the sequences with MMSeqs2 (Steinegger & Söding, 2017) into 17 million clusters and then sampled each sequence in the batch from a different cluster.

Due to the computational limitations, during training, we limited the length of the input into the language model to 1024 tokens. Every sequence begins with a [CLS] token, i.e., a classification token, and ends with an [EOS] token, i.e., an end-of-sequence token. If an input sequence is longer than 1022 nucleotides, a random part of the sequence will be cropped out and fed into the model during each epoch, similar to what was done in (Rives et al., 2021).

Once pre-trained, RiNALMo’s output embeddings can serve as a powerful sequence representation that has embedded structural and evolutionary information. Such a representation can be used as an enriched input to structural and functional downstream tasks. We employed RiNALMo in a few prediction tasks to assess its performance and generalization capabilities. However, we anticipate it can be leveraged in many other tasks related to RNA structure and function.

To qualitatively visualize pre-trained RiNALMo’s sequence representations, we employed t-SNE on the classification token embeddings for RNAs from a secondary structure prediction dataset (see Figure 2). In the output embedding space, it can be seen that the RNAs are clustered by families, and each family has a similar structure, with, in general, clean boundaries between clusters.

#### 4. Downstream Tasks

We used pre-trained RiNALMo to solve one structure and two function prediction tasks. First, we show how RiNALMo can improve secondary structure prediction. In particular, RiNALMo’s generalization capability overcomes the inability of other deep learning methods for secondary structure prediction to generalize on unseen RNA families. Second, we show that RiNALMo can be successfully utilized in multi-species splice-site and mean ribosome loading prediction tasks where it achieves state-of-the-art results. In this section, we report the most important results on the

downstream tasks, and more details and the ablation study can be found in Appendix B.

#### 4.1. Secondary Structure Prediction

When RNAs fold into complex structures, many of their bases pair up and form hydrogen bonds. These pairs are vital for the structure’s stability and function. Information about secondary structure alone can tell us a lot about the RNA and is often used as an input to the tertiary structure prediction tools.

Most popular secondary structure prediction tools often rely on thermodynamic models, aiming to identify secondary structures that possess the lowest free energy (Reuter & Mathews, 2010). There are also popular probabilistic methods based on statistical learning procedures that act as an alternative to free energy minimization methods, such as CONTRAfold (Do et al., 2006). Several deep learning methods have been developed as well, and while they outperform the thermodynamic models on RNA families on which they were trained, they are usually unable to generalize well on new families. This is a severe limitation as it hinders practical usage of such tools (Szikszai et al., 2022).

We fine-tuned RiNALMo on a simple binary classification task with binary cross-entropy loss, where we tasked the model to classify each nucleotide pair as either paired or unpaired. A simple bottleneck residual neural network (ResNet) (He et al., 2016) is attached to the language model and is fed with nucleotide pair representations obtained by doing an outer concatenation of RiNALMo’s output with itself.

First, we utilized datasets proposed in Singh et al. (2019) and compared our model to RNA-FM (Chen et al., 2022) and popular deep learning methods specialized for secondary structure prediction SPOT-RNA (Singh et al., 2019), Ufold (Fu et al., 2021) and MXfold2 (Sato et al., 2021). Proposed training and evaluation datasets are denoted as TR0 and TS0 respectively and are non-redundant to each other on the sequence similarity level. All models were trained on the same training dataset (TR0) except SPOT-RNA which was additionally fine-tuned on a smaller dataset derived from PDB (Berman et al., 2000). Notice that sequences from the same RNA family can appear in both the training and evaluation datasets. As can be seen in Table 1, RiNALMo significantly outperforms other approaches.

To test the generalization capabilities of our model, we utilized the dataset proposed in (Szikszai et al., 2022). The dataset of 3865 RNAs from nine families was split nine times, and in each split, a different family was held out for evaluation while the other eight families were used for training and validation. RiNALMo’s ability to generalize across different RNA families was compared to RNA-FM (Chen

Table 1. Performance of different models on the TS0 evaluation dataset.

MODEL	PRECISION	RECALL	F1
SPOT-RNA	0.70	0.62	0.64
UFOLD	0.63	0.71	0.66
MXFOLD2	0.67	0.57	0.60
RiNALMo	<b>0.78</b>	<b>0.73</b>	<b>0.75</b>
RNA-FM	0.71	0.66	0.68

et al., 2022), popular thermodynamics-based tool RNAs-structure (Reuter & Mathews, 2010), probabilistic method CONTRAfold (Do et al., 2006), and two deep learning approaches specialized for secondary structure prediction Ufold (Fu et al., 2021) and MXFold2 (Sato et al., 2021). The language models were fine-tuned and the other two deep learning models were separately trained on each of the previously described dataset splits and evaluated on a corresponding unseen RNA family. For predicting the secondary structures using CONTRAfold, we used EternaFold parameters (Wayment-Steele et al., 2022) trained on the EternaBench dataset, a set of more than 20,000 RNAs.

F1 scores for different dataset splits are shown in Table 2. Fine-tuned RiNALMo demonstrates that it is more than capable of inter-family generalization as it outperforms RNAs-structure in eight out of nine families by high margins, unlike other deep learning models. It is worth noting, however, that RiNALMo struggles to generalize on telomerase RNAs, but it achieves the highest F1 score on all other families. Visualization of RiNALMo’s sequence embeddings for all RNAs in the dataset is presented in Figure 2. One can notice that telomerase RNAs are clustered together, however, there is no clear boundary between them and SRP RNAs. We also noticed that telomerase RNAs are the longest in the dataset, on average around 25% longer than the second-longest in the dataset. Interestingly, Ufold performs best on telomerase RNA, while achieving much worse results on the other families. We are currently unable to conclude why RiNALMo fails on telomerase RNAs, but will take more focus on this problem in the future.

When assessing the performance of secondary structure prediction, it is important to consider RNA structural dynamics, and that’s why it is helpful to view predictions that are close enough as correct. We employed the metric calculation approach proposed in Mathews (2019). To be more precise, for a nucleotide pairing  $(i, j)$  where  $i$  and  $j$  represent nucleotide indices in the RNA sequence,  $(i \pm 1, j)$  and  $(i, j \pm 1)$  pairings are also considered correct predictions. The same approach has been utilized in both Table 1 and Table 2.

An example of secondary structure prediction from the inter-family generalization task can be seen in Figure 3. More details on the pipeline and examples of the secondary struc-

Table 2. Inter-family generalization evaluation F1 scores for secondary structure prediction.

TEST FAMILY	RNASTRUCTURE	CONTRAFOLD	RiNALMo	RNA-FM	MXFOLD2	UFOLD
5S rRNA	0.63	0.63	<b>0.88</b>	0.57	0.54	0.53
SRP RNA	0.63	0.55	<b>0.70</b>	0.25	0.50	0.26
tRNA	0.70	0.77	<b>0.93</b>	0.79	0.64	0.26
tMRNA	0.43	0.49	<b>0.80</b>	0.28	0.46	0.40
RNASE P RNA	0.55	0.63	<b>0.80</b>	0.31	0.51	0.41
GROUP I INTRON	0.54	0.60	<b>0.66</b>	0.16	0.45	0.45
16S rRNA	0.57	0.58	<b>0.74</b>	0.14	0.55	0.41
TELOMERASE RNA	0.50	0.54	0.12	0.07	0.34	<b>0.80</b>
23S rRNA	0.73	0.71	<b>0.85</b>	0.19	0.64	0.45
MEAN	0.59	0.61	<b>0.72</b>	0.31	0.51	0.44

ture prediction can be found in Appendix B.1.

## 4.2. Multi-Species Splice-Site Prediction

RNA splicing plays an important role in eukaryotic gene expression, involving the removal of introns from precursor messenger RNAs (pre-mRNAs) and the ligation of exons to form mature mRNAs. Precisely pinpointing splice sites—the donor and acceptor sites that mark the boundaries between exons and introns, and vice versa—is essential for predicting gene structure and location accurately.

Identifying the donor and acceptor sites can be cast as a binary sequence-level classification task, where a method has to detect whether a query RNA sequence contains a donor/acceptor site or not. A widely used dataset of positive and negative subsets of splice-site sequences was proposed in (Scalzitti et al., 2021). The dataset was constructed by randomly selecting sequences from the exon/intron regions of the G3PO+ genomic sequences (Scalzitti et al., 2020). The dataset consists of “confirmed” error-free splice-site sequences from a diverse set of 148 eukaryotic organisms, including humans. The test dataset consists of 4 different species not seen in the training, namely fish (*Danio rerio*), fruit fly (*Drosophila melanogaster*), worm (*Caenorhabditis elegans*) and plant (*Arabidopsis thaliana*).

We fine-tuned RiNALMo on the training dataset to predict splice sites in the sequences. The classification token (CLS) was used as input to the prediction head. This head is configured as a two-layer multilayer perceptron (MLP) featuring a hidden layer with 128 dimensions and employing the GELU activation function. Cross-entropy loss served as our choice for the loss function. We separately fine-tuned the model, first for the donor and then for the acceptor splice-site prediction task. Finally, we compared our model’s performance with other RNA language models RNA-FM (Chen et al., 2022) and Uni-RNA (Wang et al., 2023), and several established methods such as Spliceator (Scalzitti et al., 2021) and SpliceBERT (Chen et al., 2023). We used the F1 score as the evaluation metric and presented the results in Table 3.

Table 3. Classification F1 score for multi-species splice-site prediction. We report the average value of donor and acceptor prediction results. FT denotes whether we fine-tuned the model or represented direct citations from original papers with the same split train/test datasets.

MODEL	FT	FISH	FLY	PLANT	WORM
RiNALMo	✓	<b>97.70</b>	<b>96.11</b>	<b>96.25</b>	<b>95.63</b>
SPLICEBERT	✓	96.70	95.83	94.96	94.82
UNI-RNA	×	96.35	94.98	93.62	93.94
RNA-FM	✓	94.94	93.21	89.93	90.79
SPLICEATOR	×	93.50	92.91	92.85	91.60

We fine-tuned other models and used the same prediction head if they were publicly available and easy to fine-tune. Our fine-tuned model achieves state-of-the-art results in the multi-species splice-site prediction task, showing its powerful generalization properties. Notice that RiNALMo even outperforms SpliceBERT, a large language model pre-trained exclusively on pre-mRNA sequences. More details on the splice-site prediction task and the model’s hyperparameters can be found in Appendix B.2.

## 4.3. Mean Ribosome Loading Prediction

Due to efficiency reasons, cells usually use groups of multiple ribosomes to translate the mRNA. These groups are called polyribosomes, and they enable the cell to create multiple proteins from a single mRNA molecule. To quantify protein synthesis activity, a metric called mean ribosome load (MRL), defined as the average number of ribosomes that translate the mRNA instructions into polypeptides, has been introduced. MRL can provide valuable insights into various biological functions and diseases.

MRL prediction task can be viewed as a regression task where the input is the 5’ UTR region of the mRNA sequence. Commonly used datasets of 5’ UTR sequences with measured MRL values are provided by Sample et al. (2019). Two evaluation datasets were created by sampling the origi-

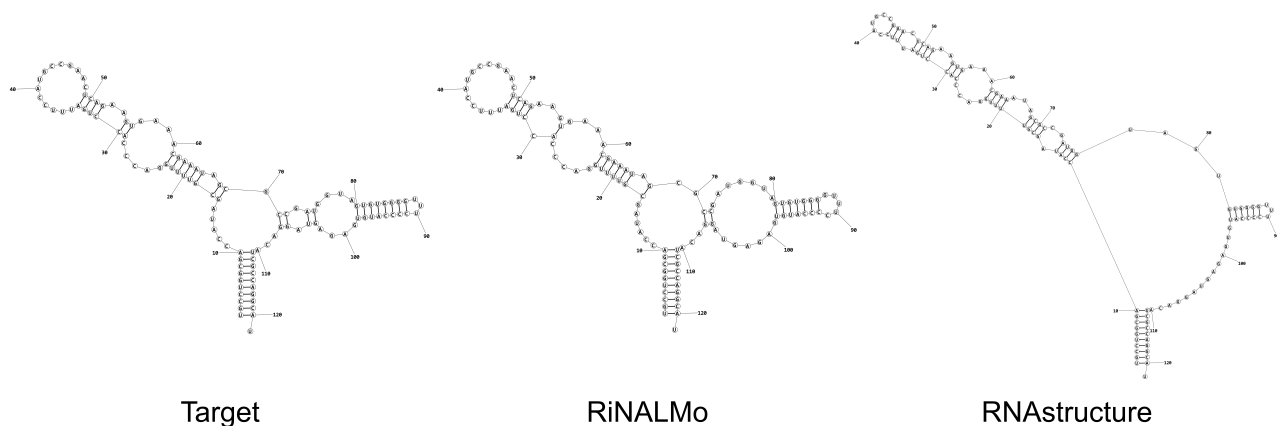


Figure 3. An example of secondary structure prediction. The shown secondary structure is a member of the 5S rRNA family and was used as a part of the evaluation dataset. RiNALMo is able to reconstruct the secondary structure accurately despite being fine-tuned with the dataset without any 5S rRNA. More examples of secondary structure predictions can be found in Appendix B.1 in Figure 5.

nal dataset that contains human and random UTR sequences of varying lengths. To ensure that each sequence length is represented equally in the dataset, 100 sequences with the deepest read coverage were selected for every length from 25 to 100 nucleotides. The same approach has been applied to both the human and random 5' UTR sequences, yielding two evaluation datasets called Random7600 and Human7600. All remaining random 5' UTRs with acceptable read coverage depth were used as the training dataset.

We fine-tuned RiNALMo on the training dataset to predict the MRL value for the given 5' UTR sequence. Language model outputs are fed into a prediction head which consists of six ResNet convolutional blocks. The mean squared error was used as the loss function. The model’s performance was compared to other RNA language models UNI-RNA (Wang et al., 2023) and RNA-FM (Chen et al., 2022). RNA-FM was fine-tuned with the same prediction head as RiNALMo. We also compared our model to the popular Optimus 5-prime model (Sample et al., 2019) specialized for MRL prediction.  $R^2$  was used as the evaluation metric, and the results are reported in Table 4. Fine-tuned RiNALMo outperforms other models. Notice that RiNALMo can generalize on human UTRs despite being fine-tuned only on sequences of random origin, proving again its generalization capability.

More details on the MRL prediction task can be found in Appendix B.3.

## 5. Discussion

We pre-trained our RNA language model on a vast amount of ncRNA sequences from several databases, including RNACentral, Rfam, nt, and Ensembl. The data was carefully curated to ensure sequence diversity in each training batch,

Table 4.  $R^2$  score for mean ribosome load prediction. FT denotes whether we trained the model or represented direct citations from original papers with the same split train/test datasets.

MODEL	FT	RANDOM7600	HUMAN7600
RiNALMo	✓	<b>0.93</b>	<b>0.86</b>
UNI-RNA	×	0.91	0.85
RNA-FM	✓	0.84	0.79
OPTIMUS 5-PRIME	✓	0.84	0.78

which subsequently led to better generalization capabilities of the pre-trained language model. We used t-SNE on the classification token embeddings to show that RiNALMo’s output representations contain information about the RNA family and that the RNAs with similar structures are close in the model’s embedding space. A more insightful way of assessing the embeddings’ expressiveness and whether the model captures hidden structure information is to assess it on downstream tasks.

First, we fine-tuned and tested RiNALMo on two secondary structure prediction tasks. The first task was an intra-family secondary structure prediction, where RNAs from the same family come in both training and test datasets. The results showed that fine-tuned RiNALMo’s output representation embeds important structure information about the input sequence and, when utilized with a proper prediction head, leads to state-of-the-art performance. The second task was an inter-family secondary structure prediction, where an RNA family from the test dataset was not seen in the training dataset. It was shown previously that deep learning methods do not generalize well across RNA families (Szikszai et al., 2022). However, RiNALMo outperformed

both thermodynamics-based and deep learning methods and showed that RNA language models can generalize well on unseen RNA families. This demonstrates the outstanding generalization capability of RiNALMo for secondary structure prediction tasks.

Furthermore, we fine-tuned RiNALMo on two function-related RNA downstream tasks. Both of these tasks were related to the mRNA family whose examples were not contained in the pre-training dataset. The results from Section 4.2 and Section 4.3 showed that RiNALMo again generalizes well and can capture important functional information from RNA sequences from previously unseen families.

In future work, we will employ RiNALMo in several other structure and function-related tasks. Of particular interest would be to test RiNALMo on tertiary structure prediction tasks and see whether its expressive output embeddings and generalization capability can improve the performance of existing or new prediction tools.

## 6. Conclusion

In this paper, we presented RiNALMo, a new largest-to-date general-purpose RNA language model pre-trained on a dataset of 36M unique ncRNA sequences using masked language modeling. We showed that by pre-training on a carefully curated RNA dataset and using the most modern Transformer modules and techniques, a language model can capture hidden knowledge and important structural information from unlabeled RNA sequences. The results of several structural and functional downstream tasks proved the generalization capability of RiNALMo and the expressiveness of its output representations. Of particular importance are the results of the inter-family secondary structure prediction task, where we showed that RiNALMo can generalize well on RNA families unseen during fine-tuning, unlike other deep learning methods. Due to the significance of the results, we believe RiNALMo presents a valuable asset for advancing our understanding of RNA structures and functions.

## Acknowledgements

The authors would like to thank Ivona Martinović for the valuable comments and fruitful discussion on this work.

This work was supported in part by the National Research Foundation (NRF) Competitive Research Programme (CRP) under Project *Identifying Functional RNA Tertiary Structures in Dengue Virus* (NRF-CRP27-2021RS-0001) and in part by the A\*STAR under Grant *GAP2: A\*STAR RNA-Foundation Model (A\*STAR RNA-FM) (I23D1AG079)*.

The computational work for this article was partially performed on resources of the National Supercomputing Centre,

Singapore (<https://www.nsc.sg>).

## Impact Statement

This paper presents work whose goal is to advance the field of Machine Learning. There are many potential societal consequences of our work, none of which we feel must be specifically highlighted here.

## References

- Berman, H. M., Westbrook, J., Feng, Z., Gilliland, G., Bhat, T. N., Weissig, H., Shindyalov, I. N., and Bourne, P. E. The Protein Data Bank. *Nucleic Acids Research*, 28(1): 235–242, 01 2000. ISSN 0305-1048. doi: 10.1093/nar/28.1.235. URL <https://doi.org/10.1093/nar/28.1.235>.
- Brandes, N., Ofer, D., Peleg, Y., Rappoport, N., and Linial, M. ProteinBERT: a universal deep-learning model of protein sequence and function. *Bioinformatics*, 38(8): 2102–2110, 2022.
- Brown, T., Mann, B., Ryder, N., Subbiah, M., Kaplan, J. D., Dhariwal, P., Neelakantan, A., Shyam, P., Sastry, G., Askell, A., et al. Language models are few-shot learners. *Advances in neural information processing systems*, 33: 1877–1901, 2020.
- Celaj, A., Gao, A. J., Lau, T. T., Holgersen, E. M., Lo, A., Lodaya, V., Cole, C. B., Denroche, R. E., Spickett, C., Wagih, O., et al. An RNA foundation model enables discovery of disease mechanisms and candidate therapeutics. *bioRxiv*, 2023. doi: 10.1101/2023.09.20.558508. URL <https://www.biorxiv.org/content/early/2023/09/26/2023.09.20.558508>.
- Chen, B., Cheng, X., Geng, Y.-a., Li, S., Zeng, X., Wang, B., Gong, J., Liu, C., Zeng, A., Dong, Y., et al. xTrimoPGLM: Unified 100B-scale pre-trained transformer for deciphering the language of protein. *Biorxiv*, 2024. doi: 10.1101/2023.07.05.547496. URL <https://www.biorxiv.org/content/early/2024/01/11/2023.07.05.547496>.
- Chen, J., Hu, Z., Sun, S., Tan, Q., Wang, Y., Yu, Q., Zong, L., Hong, L., Xiao, J., Shen, T., et al. Interpretable RNA foundation model from unannotated data for highly accurate RNA structure and function predictions. Eprint [arXiv:2204.00300](https://arxiv.org/abs/2204.00300), 2022.
- Chen, K., Zhou, Y., Ding, M., Wang, Y., Ren, Z., and Yang, Y. Self-supervised learning on millions of pre-mRNA sequences improves sequence-based RNA splicing prediction. *bioRxiv*, 2023. doi: 10.1101/2023.01.31.526427. URL <https://www.biorxiv.org/content/early/2023/02/03/2023.01.31.526427>.

- Childs-Disney, J. L., Yang, X., Gibaut, Q. M., Tong, Y., Batey, R. T., and Disney, M. D. Targeting RNA structures with small molecules. *Nature Reviews Drug Discovery*, 21(10):736–762, 2022.
- Chowdhery, A., Narang, S., Devlin, J., Bosma, M., Mishra, G., Roberts, A., Barham, P., Chung, H. W., Sutton, C., Gehrmann, S., et al. PaLM: Scaling language modeling with pathways. *Journal of Machine Learning Research*, 24(240):1–113, 2023. URL <http://jmlr.org/papers/v24/22-1144.html>.
- Dao, T. FlashAttention-2: Faster attention with better parallelism and work partitioning. Eprint [arXiv:2307.08691](https://arxiv.org/abs/2307.08691), 2023.
- Devlin, J., Chang, M.-W., Lee, K., and Toutanova, K. BERT: Pre-training of deep bidirectional transformers for language understanding. Eprint [arXiv:1810.04805](https://arxiv.org/abs/1810.04805), 2018.
- Do, C. B., Woods, D. A., and Batzoglou, S. CONTRAfold: RNA secondary structure prediction without physics-based models. *Bioinformatics*, 22(14):e90–e98, 2006. doi: 10.1093/bioinformatics/btl246. URL <https://doi.org/10.1093/bioinformatics/btl246>.
- Elnaggar, A., Heinzinger, M., Dallago, C., Rehawi, G., Wang, Y., Jones, L., Gibbs, T., Feher, T., Angerer, C., Steinegger, M., et al. ProtTrans: Toward understanding the language of life through self-supervised learning. *IEEE Transactions on Pattern Analysis and Machine Intelligence*, 44(10):7112–7127, 2022. doi: 10.1109/TPAMI.2021.3095381.
- Ferruz, N., Schmidt, S., and Höcker, B. ProtGPT2 is a deep unsupervised language model for protein design. *Nature communications*, 13(1):4348, 2022.
- Fu, L., Cao, Y., Wu, J., Peng, Q., Nie, Q., and Xie, X. Ufold: fast and accurate RNA secondary structure prediction with deep learning. *Nucleic Acids Research*, 50(3):e14–e14, 2021. doi: 10.1093/nar/gkab1074. URL <https://doi.org/10.1093/nar/gkab1074>.
- Garner, A. L. Contemporary progress and opportunities in RNA-targeted drug discovery. *ACS Medicinal Chemistry Letters*, 14(3):251–259, 2023.
- He, K., Zhang, X., Ren, S., and Sun, J. Deep residual learning for image recognition. In *Proceedings of the IEEE conference on computer vision and pattern recognition*, pp. 770–778, 2016.
- Heinzinger, M., Elnaggar, A., Wang, Y., Dallago, C., Nechaev, D., Matthes, F., and Rost, B. Modeling aspects of the language of life through transfer-learning protein sequences. *BMC bioinformatics*, 20(1):1–17, 2019.
- Ji, Y., Zhou, Z., Liu, H., and Davuluri, R. V. DNABERT: pre-trained Bidirectional Encoder Representations from Transformers model for DNA-language in genome. *Bioinformatics*, 37(15):2112–2120, Feb 2021. doi: 10.1093/bioinformatics/btab083. URL <https://doi.org/10.1093/bioinformatics/btab083>.
- Jumper, J., Evans, R., Pritzel, A., Green, T., Figurnov, M., Ronneberger, O., Tunyasuvunakool, K., Bates, R., Židek, A., Potapenko, A., et al. Highly accurate protein structure prediction with AlphaFold. *Nature*, 596(7873):583–589, 2021.
- Kalvari, I., Nawrocki, E. P., Ontiveros-Palacios, N., Argasinska, J., Lamkiewicz, K., Marz, M., Griffiths-Jones, S., Toffano-Nioche, C., Gautheret, D., Weinberg, Z., et al. Rfam 14: expanded coverage of metagenomic, viral and microRNA families. *Nucleic Acids Research*, 49(D1):D192–D200, 2020. doi: 10.1093/nar/gkaa1047. URL <https://doi.org/10.1093/nar/gkaa1047>.
- Lin, Z., Akin, H., Rao, R., Hie, B., Zhu, Z., Lu, W., Smetanin, N., Verkuil, R., Kabeli, O., Shmueli, Y., et al. Evolutionary-scale prediction of atomic-level protein structure with a language model. *Science*, 379(6637):1123–1130, 2023. doi: 10.1126/science.ade2574. URL <https://www.science.org/doi/abs/10.1126/science.ade2574>.
- Madani, A., Krause, B., Greene, E. R., Subramanian, S., Mohr, B. P., Holton, J. M., Olmos Jr, J. L., Xiong, C., Sun, Z. Z., Socher, R., et al. Large language models generate functional protein sequences across diverse families. *Nature Biotechnology*, 41:1099–1106, 2023.
- Martin, F. J., Amode, M. R., Aneja, A., Austine-Orimoloye, O., Azov, A. G., Barnes, I., Becker, A., Bennett, R., Berry, A., Bhai, J., et al. Ensembl 2023. *Nucleic Acids Research*, 51(D1):D933–D941, 2022. doi: 10.1093/nar/gkac958. URL <https://doi.org/10.1093/nar/gkac958>.
- Mathews, D. H. How to benchmark RNA secondary structure prediction accuracy. *Methods*, 162-163:60–67, 2019. doi: <https://doi.org/10.1016/j.ymeth.2019.04.003>. URL <https://www.sciencedirect.com/science/article/pii/S1046202318303402>.
- McWhite, C. D., Armour-Garb, I., and Singh, M. Leveraging protein language models for accurate multiple sequence alignments. *Genome Research*, 33(7):1145–1153, 2023.
- Nambiar, A., Heflin, M., Liu, S., Maslov, S., Hopkins, M., and Ritz, A. Transforming the language of life: transformer neural networks for protein prediction tasks. In *Proceedings of the 11th ACM International Conference*

- on *Bioinformatics, Computational Biology and Health Informatics*, pp. 1–8, 2020.
- Nijkamp, E., Ruffolo, J. A., Weinstein, E. N., Naik, N., and Madani, A. ProGen2: exploring the boundaries of protein language models. *Cell Systems*, 14(11):968–978, 2023.
- Paszke, A., Gross, S., Massa, F., Lerer, A., Bradbury, J., Chanan, G., Killeen, T., Lin, Z., Gimelshein, N., Antiga, L., et al. Pytorch: An imperative style, high-performance deep learning library. In *Advances in Neural Information Processing Systems 32*, pp. 8024–8035, 2019.
- Radford, A., Narasimhan, K., Salimans, T., Sutskever, I., et al. Improving language understanding by generative pre-training. 2018.
- Raffel, C., Shazeer, N., Roberts, A., Lee, K., Narang, S., Matena, M., Zhou, Y., Li, W., and Liu, P. J. Exploring the limits of transfer learning with a unified text-to-text transformer. *The Journal of Machine Learning Research*, 21(1):5485–5551, 2020.
- Reuter, J. S. and Mathews, D. H. RNAstructure: software for RNA secondary structure prediction and analysis. *BMC Bioinformatics*, 11:129, 2010.
- Rives, A., Meier, J., Sercu, T., Goyal, S., Lin, Z., Liu, J., Guo, D., Ott, M., Zitnick, C. L., Ma, J., et al. Biological structure and function emerge from scaling unsupervised learning to 250 million protein sequences. *Proceedings of the National Academy of Sciences*, 118(15):e2016239118, 2021.
- RNAcentral Consortium. RNAcentral 2021: secondary structure integration, improved sequence search and new member databases. *Nucleic Acids Research*, 49(D1):D212–D220, 2020. doi: 10.1093/nar/gkaa921. URL <https://doi.org/10.1093/nar/gkaa921>.
- Sample, P. J., Wang, B., Reid, D. W., Presnyak, V., McFadyen, I. J., Morris, D. R., and Seelig, G. Human 5' UTR design and variant effect prediction from a massively parallel translation assay. *Nature Biotechnology*, 37(7):803–809, Jul 2019. doi: 10.1038/s41587-019-0164-5. URL <https://doi.org/10.1038/s41587-019-0164-5>.
- Sato, K., Akiyama, M., and Sakakibara, Y. RNA secondary structure prediction using deep learning with thermodynamic integration. *Nature Communications*, 12(1):941, Feb 2021. doi: 10.1038/s41467-021-21194-4. URL <https://doi.org/10.1038/s41467-021-21194-4>.
- Sayers, E. W., Bolton, E. E., Brister, J. R., Canese, K., Chan, J., Comeau, D. C., Farrell, C. M., Feldgarden, M., Fine, A. M., Funk, K., et al. Database resources of the National Center for Biotechnology Information in 2023. *Nucleic Acids Research*, 51(D1):D29–D38, 2022. doi: 10.1093/nar/gkac1032. URL <https://doi.org/10.1093/nar/gkac1032>.
- Scalzitti, N., Jeannin-Girardon, A., Collet, P., Poch, O., and Thompson, J. D. A benchmark study of ab initio gene prediction methods in diverse eukaryotic organisms. *BMC Genomics*, 21:1–20, 2020.
- Scalzitti, N., Kress, A., Orhand, R., Weber, T., Moulinier, L., Jeannin-Girardon, A., Collet, P., Poch, O., and Thompson, J. D. Spliceator: Multi-species splice site prediction using convolutional neural networks. *BMC Bioinformatics*, 22(1):1–26, 2021.
- Shazeer, N. GLU variants improve transformer. Eprint [arXiv:2002.05202](https://arxiv.org/abs/2002.05202), 2020.
- Shen, T., Hu, Z., Peng, Z., Chen, J., Xiong, P., Hong, L., Zheng, L., Wang, Y., King, I., Wang, S., et al. E2Efold-3D: end-to-end deep learning method for accurate de novo RNA 3D structure prediction. Eprint [arXiv:2207.01586](https://arxiv.org/abs/2207.01586), 2022.
- Singh, J., Hanson, J., Paliwal, K., and Zhou, Y. RNA secondary structure prediction using an ensemble of two-dimensional deep neural networks and transfer learning. *Nature Communications*, 10(1):5407, Nov 2019. doi: 10.1038/s41467-019-13395-9. URL <https://doi.org/10.1038/s41467-019-13395-9>.
- Steinegger, M. and Söding, J. MMseqs2 enables sensitive protein sequence searching for the analysis of massive data sets. *Nature Biotechnology*, 35(11):1026–1028, 2017. doi: 10.1038/nbt.3988. URL <https://doi.org/10.1038/nbt.3988>.
- Su, J., Ahmed, M., Lu, Y., Pan, S., Bo, W., and Liu, Y. RoFormer: Enhanced transformer with rotary position embedding. *Neurocomputing*, 568:127063, 2024.
- Szicszai, M., Wise, M., Datta, A., Ward, M., and Mathews, D. H. Deep learning models for RNA secondary structure prediction (probably) do not generalize across families. *Bioinformatics*, 38(16):3892–3899, 2022. doi: 10.1093/bioinformatics/btac415. URL <https://doi.org/10.1093/bioinformatics/btac415>.
- Touvron, H., Lavril, T., Izacard, G., Martinet, X., Lachaux, M.-A., Lacroix, T., Rozière, B., Goyal, N., Hambro, E., Azhar, F., et al. Llama: Open and efficient foundation language models. *arXiv preprint arXiv:2302.13971*, 2023.
- Vaswani, A., Shazeer, N., Parmar, N., Uszkoreit, J., Jones, L., Gomez, A. N., Kaiser, Ł., and Polosukhin, I. Attention is all you need. *Advances in neural information processing systems*, 30, 2017.

- Wang, X., Gu, R., Chen, Z., Li, Y., Ji, X., Ke, G., and Wen, H. Uni-RNA: Universal pre-trained models revolutionize RNA research. *bioRxiv*, 2023. doi: 10.1101/2023.07.11.548588. URL <https://www.biorxiv.org/content/early/2023/07/12/2023.07.11.548588>.
- Wayment-Steele, H. K., Kladwang, W., Strom, A. I., Lee, J., Treuille, A., Becka, A., Participants, E., and Das, R. RNA secondary structure packages evaluated and improved by high-throughput experiments. *Nature Methods*, 19(10): 1234–1242, 2022.
- Wu, R., Ding, F., Wang, R., Shen, R., Zhang, X., Luo, S., Su, C., Wu, Z., Xie, Q., Berger, B., et al. High-resolution de novo structure prediction from primary sequence. *bioRxiv*, 2022. doi: 10.1101/2022.07.21.500999. URL <https://www.biorxiv.org/content/early/2022/07/22/2022.07.21.500999>.
- Xiong, R., Yang, Y., He, D., Zheng, K., Zheng, S., Xing, C., Zhang, H., Lan, Y., Wang, L., and Liu, T. On layer normalization in the transformer architecture. In *International Conference on Machine Learning*, pp. 10524–10533. PMLR, 2020.
- Yang, F., Wang, W., Wang, F., Fang, Y., Tang, D., Huang, J., Lu, H., and Yao, J. scBERT as a large-scale pretrained deep language model for cell type annotation of single-cell RNA-seq data. *Nature Machine Intelligence*, 4:852–866, 2022.
- Zhang, T., Singh, J., Litfin, T., Zhan, J., Paliwal, K., and Zhou, Y. RNACmap: a fully automatic pipeline for predicting contact maps of RNAs by evolutionary coupling analysis. *Bioinformatics*, 37(20): 3494–3500, 05 2021. doi: 10.1093/bioinformatics/btab391. URL <https://doi.org/10.1093/bioinformatics/btab391>.
- Zhang, Y., Lang, M., Jiang, J., Gao, Z., Xu, F., Litfin, T., Chen, K., Singh, J., Huang, X., Song, G., et al. Multiple sequence alignment-based RNA language model and its application to structural inference. *Nucleic Acids Research*, 52(1):e3–e3, 11 2024. doi: 10.1093/nar/gkad1031. URL <https://doi.org/10.1093/nar/gkad1031>.
- Zhou, Z., Ji, Y., Li, W., Dutta, P., Davuluri, R., and Liu, H. DNABERT-2: Efficient foundation model and benchmark for multi-species genome. Eprint [arXiv:2306.15006](https://arxiv.org/abs/2306.15006), 2023.

Table 5. Language model configurations and their hyperparameters.

HYPERPARAMETER	RiNALMo-135M	RiNALMo-650M
LAYERS	30	33
EMBED. DIM.	640	1280
ATTENTION HEADS	20	20
ROPE	TRUE	TRUE
ATTENTION DROPOUT	0.1	0.1
RESIDUAL DROPOUT	0.1	0.1

## A. RNA language model

Data pre-processing consists of replacing all “U”s in the sequences with “T”s. This leads to a vocabulary involving four main types of nucleotides (“A”, “C”, “T” and “G”) and several other types of combinations (“I”, “R”, “V”, “K”, “M”, “S”, “W”, “B”, “D”, “H”, “V”, “N”, and “-”). Additionally, we use several other tokens used commonly in MLM, such as [CLS], [EOS], [PAD], and [MASK]. During masking, we change nucleotides with the [MASK] token or replace it with one of the four main types of nucleotides from the vocabulary or the “any nucleotide” (“N”) token.

RiNALMo is pre-trained using a self-supervision objective. Given an input sequence  $\mathbf{X} = \{x_i\}$ , we corrupt it by masking 15% of its tokens at random, such as described in Section 3. Let us denote the corrupted sequence by  $\tilde{\mathbf{X}} = \{\tilde{x}_i\}$ . We train RiNALMo parameterized by  $\theta$  to reconstruct  $\mathbf{X}$  by predicting the masked tokens conditioned on  $\tilde{\mathbf{X}}$ . For a given input token  $\tilde{x}_i$ , the loss is the probability of the correct nucleotide, given  $\tilde{\mathbf{X}}$ :

$$\mathcal{L}_{MLM} = -\log p_{\theta}(\tilde{x}_i = x_i | \tilde{\mathbf{X}}).$$

The weight updates are based on the average loss over the sampled tokens from a single training sequence (or a batch of sequences):

$$\mathcal{L}_{MLM} = -\frac{1}{|\mathcal{M}|} \sum_{i \in \mathcal{M}} \log p_{\theta}(\tilde{x}_i = x_i | \tilde{\mathbf{X}}),$$

where  $\mathcal{M}$  is the index set of masked tokens.

We trained two configurations of the language model: one with 650M parameters and one with 135M parameters. Model hyperparameters can be found in Table 5.

We pre-trained RiNALMo on seven A100 GPUs of 80 GB memory for 6 epochs. The batch size was set to 192 per GPU. We adopted the cosine annealing learning rate schedule with a linear warm-up. During the warm-up period, learning rate increases from  $10^{-7}$  to  $5 \times 10^{-5}$  for 2000 steps. For the cosine annealing schedule, the minimum learning rate was set to  $10^{-5}$ .

## B. Downstream Tasks

Here we provide more details on the training and fine-tuning parameters as well as the ablation study for all the downstream tasks. Additionally, we try to illustrate and give more insights into the biological background for every downstream task.

### B.1. Secondary Structure Prediction

An example of secondary structure and the secondary structure prediction using pre-trained RiNALMo are illustrated in Figure 4. The prediction head consists of two bottleneck residual blocks and its parameters were initialized with the default Pytorch (Paszke et al., 2019) parameter initialization method.

Pair representations are obtained by applying outer concatenation to RiNALMo’s output. For example, to obtain the vector representation of the nucleotide pair  $(i, j)$ , we simply concatenate the representation of the nucleotide  $j$  to the representation of the nucleotide  $i$ .

In the end, our secondary structure prediction pipeline outputs a matrix where each element represents a pairing probability logit for a certain nucleotide pair. Because of the symmetry of secondary structures (if nucleotide  $i$  is paired with nucleotide  $j$ , then  $j$  is paired with  $i$  as well), we calculate training loss only on matrix elements “above” the main diagonal.

Table 6. Inter-family generalization evaluation sequence length weighted F1 scores for secondary structure prediction.

TEST FAMILY	RiNALMo		RNASTRUCTURE		SEQUENCE LENGTH	
	F1 <sub>WEIGHTED</sub>	F1 <sub>NON-WEIGHTED</sub>	F1 <sub>WEIGHTED</sub>	F1 <sub>NON-WEIGHTED</sub>	MEAN	STD
5S rRNA	<b>0.884</b>	<b>0.884</b>	0.630	0.628	118.71	3.49
SRP RNA	0.628	<b>0.700</b>	<b>0.631</b>	0.633	180.23	100.81
TRNA	<b>0.932</b>	<b>0.931</b>	0.703	0.704	77.10	5.02
TMRNA	<b>0.802</b>	<b>0.801</b>	0.431	0.433	366.02	27.72
RNASE P RNA	<b>0.803</b>	<b>0.798</b>	0.555	0.552	332.16	49.53
GROUP I INTRON	<b>0.675</b>	<b>0.657</b>	0.542	0.535	374.59	88.58
16S rRNA	<b>0.721</b>	<b>0.736</b>	0.525	0.570	317.04	145.61
TELOMERASE RNA	0.119	0.120	<b>0.498</b>	<b>0.500</b>	438.43	28.01
23S rRNA	<b>0.840</b>	<b>0.848</b>	0.716	0.730	326.20	51.95
MEAN	0.712	0.719	0.581	0.587	281.16	55.64

During fine-tuning, we utilized gradual parameter unfreezing. After every three epochs, we unfroze additional 3 RiNALMo’s layers. In the first three epochs, we trained only the prediction head. The model was fine-tuned for 15 epochs and the learning rate was initially set to  $10^{-4}$  with a linear decay schedule. We used the same prediction head architecture for RNA-FM fine-tuning. Due to architectural differences between RiNALMo and RNA-FM, we decided to modify the fine-tuning schedule. The prediction head was first pre-trained while RNA-FM parameters were kept frozen. After three epochs we unfroze RNA-FM and fine-tuned it alongside the prediction head.

To convert base pairing probabilities to a proper secondary structure, we implemented a simple greedy approach where we iteratively set nucleotide pairs with the highest pairing probability as paired and then excluded all possible clashing pairs from being set as paired in future iterations of the algorithm. During this procedure, we ignore non-canonical nucleotide pairings and pairings that would cause a "sharp" hairpin loop ( $i$ -th nucleotide cannot be paired with the  $j$ -th nucleotide if  $|i - j| < 4$ ). The classification threshold was tuned on the validation set to ensure a balanced pairing ratio.

We trained and evaluated our model on data splits provided by (Szikszai et al., 2022). There are nine data splits based on different RNA families, for each data split one family is used for evaluation, while the other eight are used for training and validation. Data splits are denoted by the RNA family used for evaluation. For example, a 5S data split means that samples from the 5S family were held out for evaluation.

Figure 5 shows the secondary structure for one sample from each data split. Target secondary structures and predictions by both RiNALMo and RNAstructure are shown in each row.

To assess the model’s ability to accurately predict secondary structures for longer RNA sequences we also considered a weighted F1 score. To clarify, when calculating the average F1 score we weighted each score with the length of the corresponding RNA sequence. A comparison of weighted and non-weighted F1 scores on each RNA family during inter-family generalization is shown in Table 6. Notice that RiNALMo’s performance significantly drops on longer SRP RNAs but it holds up on longer sequences of all other families.

Secondary structures have been visualized with *forna*<sup>1</sup> and RNAstructure’s *draw*<sup>2</sup> utility tool.

## B.2. Multi-Species Splice-Site Prediction

We used the dataset denoted as GS.1 in the paper it was proposed in (Scalzitti et al., 2021). GS.1 has the same ratio of positive to negative samples, whose negative samples consist of exon, intron, or false positive sequences. The length of the input sequences was set to 400 nucleotides for both the training and test datasets.

The process of RNA splicing and the splice-site prediction using pre-trained RiNALMo are illustrated in Figure 6. Since RiNALMo output embeddings contain the classification token (CLS), we utilized it in the binary classification task of splice-site prediction. The prediction head was uniformly initialized from  $\mathcal{U}(-\sqrt{1/d}, \sqrt{1/d})$ , where  $d$  is the input features dimension. The learning rate was set to  $10^{-5}$  and the language model with the prediction head was fine-tuned for 2 epochs

<sup>1</sup><http://rna.tbi.univie.ac.at/forna/>

<sup>2</sup><https://rna.urmc.rochester.edu/Text/draw.html>

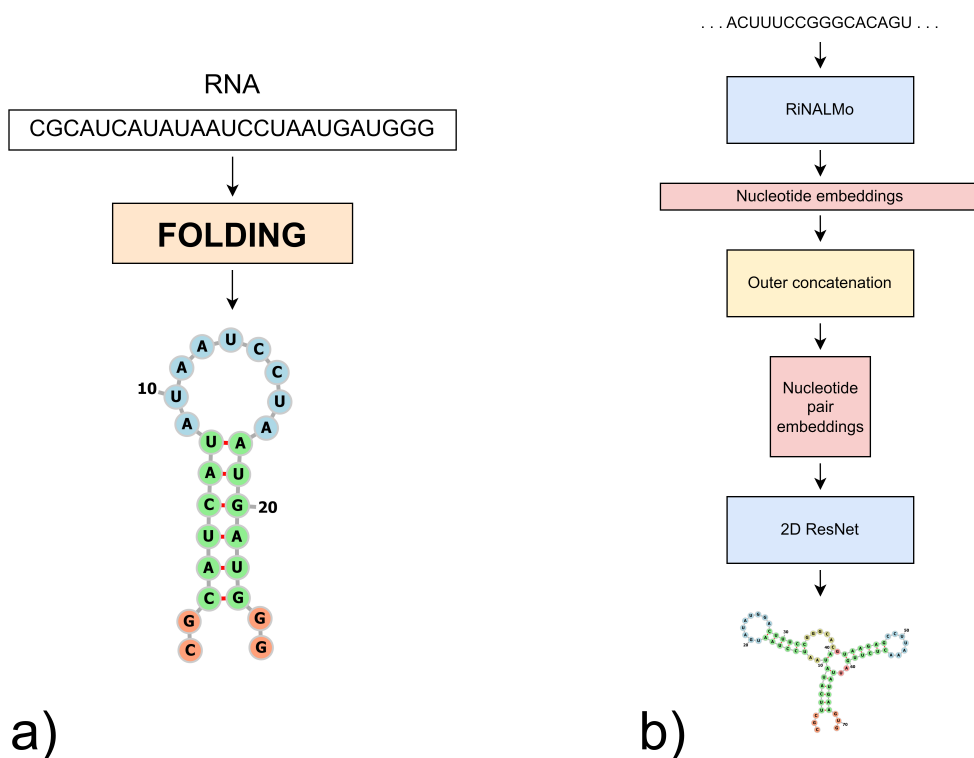


Figure 4. a) **RNA secondary structure.** RNAs fold into various shapes according to their function and while doing so, many of their nucleotides pair up using a hydrogen bond. These pairings are crucial for structure stability and form various structural motifs such as hairpin loops and bulges. b) **RNA secondary structure prediction.** Firstly, RiNALMo produces nucleotide embeddings for the given RNA sequence. Nucleotide pair embeddings are created by applying outer concatenation to RiNALMo’s outputs. Finally, pair representations are fed into the convolutional bottleneck ResNet which produces base pairing probabilities that are then converted into the final secondary structure prediction.

when it achieved the best results on the validation dataset. The batch size was set to 32.

We fine-tuned the pre-trained SpliceBERT<sup>3</sup>, and we fine-tuned the pre-trained RNA-FM model<sup>4</sup> in combination with a two-layer MLP prediction head. We fine-tuned the models on the same training/validation dataset used for fine-tuning RiNALMo with the same learning rate.

Separate classification F1 scores for donor and acceptor splice-site prediction can be found in Table 7 and Table 8, respectively. Table 3 is the mean value of results reported in Table 7 and Table 8. Notice that RiNALMo outperforms other models for both donor and acceptor site prediction in all of the columns.

### B.3. Mean Ribosome Loading Prediction

RNA translation process and the MRL prediction using pre-trained RiNALMo are illustrated in Figure 7. The prediction head is built of six convolutional blocks. Each block consists of two convolution layers followed by instance normalization and ELU activation function. Parameters of the prediction head were initialized with the default Pytorch (Paszke et al., 2019) parameter initialization method.

All MRL targets were standardized with the mean and standard deviation of training MRL values.

The model was fine-tuned for 50 epochs. In the first 5 epochs of the training, only the prediction head was trained. The learning rate was set to  $10^{-4}$  and linearly decayed to  $10^{-5}$  over the first 5000 training steps after which it remained constant. The batch size was set to 64. RNA-FM was fine-tuned with the same training procedure.

<sup>3</sup><https://github.com/biomed-AI/SpliceBERT>

<sup>4</sup><https://github.com/ml4bio/RNA-FM>

Table 7. Classification F1 score for donor splice-site prediction. FT denotes whether we fine-tuned the model or represented direct citations from original papers with the same split train/test datasets. “-” denotes that the result was not reported in the original paper.

MODEL	FT	FISH	FLY	PLANT	WORM
RiNALMo	✓	<b>97.93</b>	<b>96.38</b>	<b>97.12</b>	<b>96.40</b>
SPLICEBERT	✓	97.47	96.25	95.13	95.14
UNI-RNA	×	-	-	-	-
RNA-FM	✓	96.15	94.46	92.08	92.09
SPLICEATOR	×	95.10	94.80	94.90	94.10

Table 8. Classification F1 score for acceptor splice-site prediction. FT denotes whether we fine-tuned the model or represented direct citations from original papers with the same split train/test datasets. “-” denotes that the result was not reported in the original paper.

MODEL	FT	FISH	FLY	PLANT	WORM
RiNALMo	✓	<b>97.47</b>	<b>95.83</b>	<b>95.38</b>	<b>94.86</b>
SPLICEBERT	✓	95.93	95.41	94.78	94.50
UNI-RNA	×	-	-	-	-
RNA-FM	✓	93.72	91.95	87.78	89.49
SPLICEATOR	×	91.90	91.00	90.80	89.10

#### B.4. Ablation Study

Here, we provide ablation study results evaluated on the downstream tasks. We study the effect of a few design and learning strategy choices. First, we compare the 650 million parameters RiNALMo with a smaller 135 million parameters RiNALMo which we denote as RiNALMo-135M. RiNALMo-135M differs from RiNALMo in that it has 30 attention heads and embedding dimensionality of 640 compared to 33 and 1280 in RiNALMo. Notice that RNA-FM (Chen et al., 2022) is a 100 million parameters language model with the same dimension of embeddings. RiNALMo-135M was fine-tuned on the training datasets the same way as RiNALMo on all of the downstream tasks. Second, we want to assess the influence of fine-tuning on the performance of RiNALMo on downstream tasks. To that end, we evaluate pre-trained and frozen RiNALMo, denoted as RiNALMo-frozen, on the downstream tasks. We utilize the output embeddings of RiNALMo-frozen as an input to the prediction heads for the downstream tasks.

The ablation study results evaluated on the secondary structure prediction tasks are given in Table 9 and Table 10, on the multi-species splice-site prediction task in Table 11, and on the mean ribosome load prediction task in Table 12. It can be seen that for all of the downstream tasks RiNALMo-135M outperforms RNA-FM. We believe this is mainly due to the more sophisticated Transformer architecture and more advanced techniques such as the RoPE and the SwiGLU activation function. Analogously, one can see that RiNALMo outperforms RiNALMo-135M in almost all of the downstream tasks except for a few families in Table 9 where they perform in par. This backs the usage of the larger RiNALMo model since it generally outperforms smaller RiNALMo-135M and RNA-FM.

RiNALMo-frozen used the same prediction head as the other models in the downstream tasks but is the only one that was not fine-tuned. In Table 9, it can be seen that most of the time RiNALMo-frozen is comparable to RiNALMo on the inter-family secondary structure prediction task, but is highly outperformed by the fine-tuned model for 23S rRNA and 16S rRNA families. Furthermore, RiNALMo-frozen outperforms RNA-FM on the inter-family secondary structure prediction task by a high margin. We can conclude that pre-trained RiNALMo captures much more structural information and knowledge than concurrent RNA-FM since it already performs comparable to the fine-tuned RiNALMo model and RNA-FM is nowhere near. We can relate the generalization capability of language models for the inter-family secondary structure prediction tasks to the quality of pre-training. However, we see that fine-tuning can still lift the performance on the inter-family secondary structure prediction task. When tested on the intra-family secondary structure prediction task (Table 10) and function prediction tasks (Tables 11 and 12), it can be seen that the fine-tuned models outperform RiNALMo-frozen. There are two reasons for that. First, in the intra-family secondary structure prediction task the generalization capability of the model is not that important since the same RNA families can be seen in both training and test datasets. Second, RiNALMo is pre-trained on ncRNAs and the function prediction tasks are related to mRNAs that were not seen in the pre-training dataset. Fine-tuned models can better capture relations within RNA sequences that were not seen in pre-training.

Table 9. Inter-family generalization evaluation F1 scores for secondary structure prediction.

TEST FAMILY	RiNALMo	RiNALMo-FROZEN	RiNALMo-135M	RNA-FM
5S rRNA	<b>0.88</b>	0.86	0.85	0.57
SRP RNA	<b>0.70</b>	<b>0.70</b>	0.58	0.25
tRNA	0.93	<b>0.95</b>	0.91	0.79
TMRNA	0.80	0.79	<b>0.81</b>	0.28
RNASE P RNA	<b>0.80</b>	0.77	0.77	0.31
GROUP I INTRON	0.66	<b>0.67</b>	0.39	0.16
16S rRNA	<b>0.74</b>	0.68	0.72	0.14
TELOMERASE RNA	<b>0.12</b>	<b>0.12</b>	0.08	0.07
23S rRNA	0.85	0.72	<b>0.86</b>	0.19
MEAN	<b>0.71</b>	0.70	0.66	0.31

Table 10. Performance of different models on SPOT-RNA’s test dataset.

MODEL	PRECISION	RECALL	F1
RiNALMo	<b>0.784</b>	<b>0.730</b>	<b>0.747</b>
RiNALMo-FROZEN	0.663	0.663	0.652
RiNALMo-135M	0.755	0.711	0.723
RNA-FM	0.709	0.664	0.676

Table 11. Classification F1 score for multi-species splice-site prediction. We report the average value of donor and acceptor prediction results.

MODEL	FISH	FLY	PLANT	WORM
RiNALMo	<b>97.47</b>	<b>95.83</b>	<b>95.38</b>	<b>94.86</b>
RiNALMo-FROZEN	81.02	68.18	67.73	63.75
RiNALMo-135M	95.96	93.80	93.35	92.81
RNA-FM	94.94	93.21	89.93	90.79

Table 12.  $R^2$  score and mean absolute error (MAE) for mean ribosome loading prediction for Random7600 and Human7600 datasets.

MODEL	RANDOM7600		HUMAN7600	
	$R^2 \uparrow$	MAE $\downarrow$	$R^2 \uparrow$	MAE $\downarrow$
RiNALMo	<b>0.925</b>	<b>0.282</b>	<b>0.860</b>	<b>0.324</b>
RiNALMo-FROZEN	0.610	0.626	0.675	0.487
RiNALMo-135M	0.908	0.315	0.836	0.351
RNA-FM	0.842	0.404	0.790	0.396

## RiNALMo: RiboNucleic Acid Language Model

Test Family	Target	RNAstructure	RiNALMo
5S rRNA		 F1 = 0.70	 F1 = 0.93
SRP RNA		 F1 = 0.92	 F1 = 0.91
IRNA		 F1 = 0.55	 F1 = 0.98
tmRNA		 F1 = 0.41	 F1 = 0.91
RNase P RNA		 F1 = 0.73	 F1 = 0.92
Group I intron		 F1 = 0.78	 F1 = 0.81
16S rRNA		 F1 = 0.71	 F1 = 0.88
23S RNA		 F1 = 0.88	 F1 = 0.90
Telomerase RNA		 F1 = 0.57	 F1 = 0.19

Figure 5. **Secondary structure prediction examples.** Target secondary structures and predictions by RiNALMo and RNAstructure. The F1 score is shown in the upper right corner of each predicted structure figure.

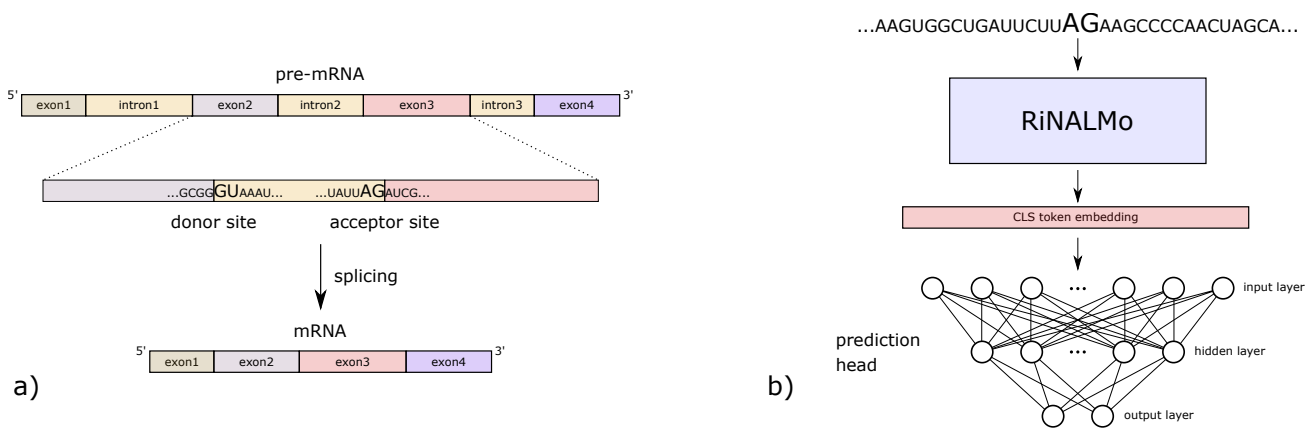


**Figure 6. a) RNA splicing.** A pre-mRNA transcript consists of non-coding, i.e., introns, and coding regions, i.e., exons. Introns are located between two exons of a gene. As part of the RNA processing pathway, introns are removed by cleavage at splice sites. These sites are found at 5' and 3' ends of introns, known as donor and acceptor splice sites, respectively. Most frequently, the 5' end of introns begins with the dinucleotide GU, and the 3' end of introns ends with AG. **b) RNA splice-site prediction.** An input to RiNALMo is a 400 nucleotide long RNA sequence. RiNALMo outputs 402 embeddings including the CLS embedding. We utilize only the CLS embedding that then passes through a two-layer MLP prediction head to determine whether a sequence contains a donor/acceptor site or not.

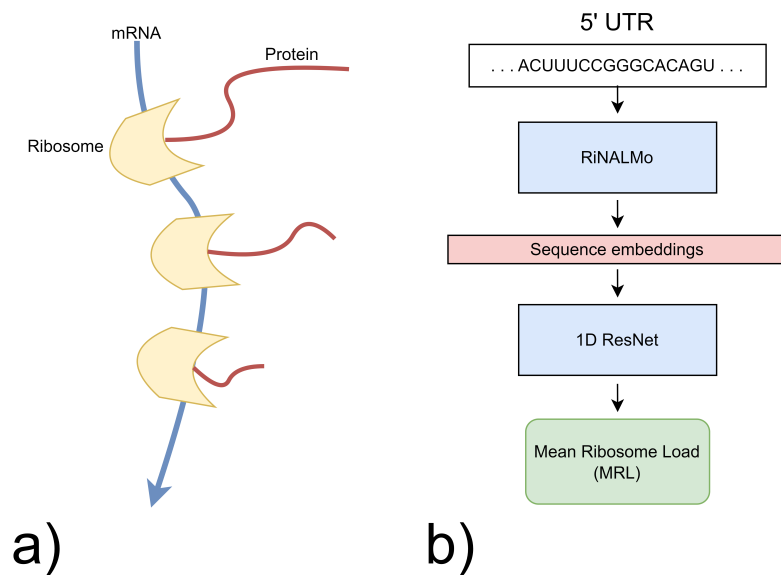


**Figure 7. a) RNA translation.** To produce multiple proteins from a single mRNA strand, cells utilize multiple ribosomes. The mean ribosome load (MRL) metric was designed to indicate the translation efficiency of a certain mRNA. **b) Mean ribosome load prediction.** Embeddings produced by RiNALMo are forwarded to the one-dimensional convolutional ResNet which outputs the mean ribosome load prediction.